Thermal noise of microcantilevers in viscous fluids

Ludovic Bellon

Thermal noise of microcantilevers in viscous fluids

L. Bellon

Université de Lyon

Laboratoire de Physique, ENS Lyon, CNRS UMR5672

46 allée d'Italie, 69364 Lyon Cedex 07, France

Ludovic.Bellon@ens-lyon.fr

November 20, 2008

Abstract

We present a simple theoretical framework to describe the thermal noise of a microscopic mechanical beam in a viscous fluid: we use the Sader approach to describe the effect of the surrounding fluid (added mass and viscous drag), and the fluctuation dissipation theorem for each flexural modes of the system to derive a general expression for the power spectrum density of fluctuations. This prediction is compared with an experimental measurement on a commercial atomic force microscopy cantilever in a frequency range covering the two first resonances. A very good agreement is found on the whole spectrum, with no adjustable parameters but the thickness of the cantilever.

1 Introduction

Cantilevers of micrometer size are nowadays present in many applications, ranging from chemical and biological sensors [1] to scanning probe microscopy [2]. In many cases, these tiny mechanical systems operate in a fluid environment (air or water for instance) which has a great influence on their dynamical behavior: the viscosity of the medium will broaden the structural resonances while the added mass due to the fluid moving along with the cantilever will shift their frequencies. A few theoretical models have been proposed to account for these effects [3–12], and validated experimentally [9–15]. Among the prediction of these approaches, the power spectrum of thermal noise induced fluctuations is of particular interest for its applications in atomic force microscopy (AFM) or micro-electromechanical systems (MEMS). We will focus here on the approach by Sader et al. [3, 5, 8], and derive a generic formula for the thermal noise using the fluctuation dissipation theorem for each mode, extending the work of Paul and Cross [4] in a simpler framework than Dorignac et al. [7]. This careful analysis is indeed incorrect in the original work of Sader et al., as noted by Paul and Cross [4], Dorignac et al. [7] and Sader et al. themselves (see ref. 44 of [5]). We will then compare the prediction of the model to a noise measurement on a commercial AFM cantilever in air: an excellent agreement is obtained for the full frequency behavior of the two first resonances, as well as at low frequencies and in the intermediate region between the two pics.

2 Theory

We will first recall the general theory to describe the motion of a cantilever immersed in a viscous fluid and subject to an arbitrary external forcing, using the same notations and approach as J. Sader [3], and then derive the expression for the thermal noise of the mechanical system. The cantilever is sketched on Fig.1. Its length L is supposed to be much larger than its width b, which itself is much larger than its thickness h. We will limit ourself in this study to the flexural modes of the cantilever: the deformations are supposed to be only perpendicular to its length (along axis z of Fig.1) and uniform across its width. Theses deformation can thus be described by the deflection $w(x,t)$, x being the spacial coordinate along the beam normalized by L, and t the time. The equation of describing the dynamics of w is [16]:

$$\frac{EI}{L^4}\frac{\partial^4 w(x,t)}{\partial x^4} + \mu\frac{\partial^2 w(x,t)}{\partial t^2} = F(x,t) \tag{1}$$
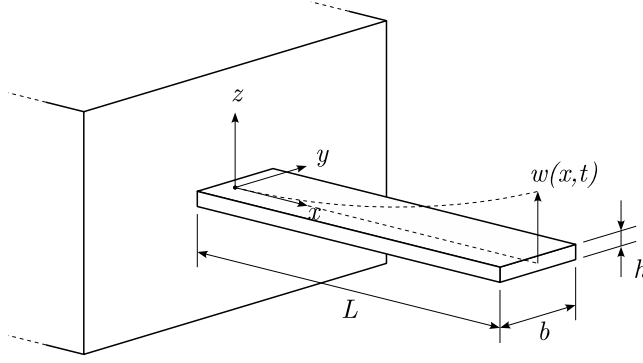
Figure 1: Geometrical model for the cantilever: rectangular beam with length L, width b and thickness h. Deformation are supposed to be only along axis z and to depend only of time t and spacial coordinate x, they are described by the deflection $w(x,t)$.

where E is the Young modulus, $I = bh^3/12$ the second moment of inertia of the cantilever, μ the mass per unit length and F the external force per unit length. The boundary conditions for eq. 1 correspond to the classical clamped ($x = 0$) and free end ($x = 1$) conditions:

$$w(x=0, t) = 0 \qquad\qquad \left.\frac{\partial w(x,t)}{\partial x}\right|_{x=0} = 0 \tag{2}$$

$$\left.\frac{\partial^2 w(x,t)}{\partial x^2}\right|_{x=1} = 0 \qquad\qquad \left.\frac{\partial^3 w(x,t)}{\partial x^3}\right|_{x=1} = 0 \tag{3}$$

In the Fourier space, we can rewrite eq. 1 as

$$\frac{k}{3}\frac{d^4 w(x|\omega)}{dx^4} - m_c\omega^2 w(x|\omega) = F(x|\omega)L \tag{4}$$

with ω the pulsation in the Fourier space, $m_c = \mu L$ the mass and $k = 3EI/L^3$ the spring constant of the cantilever. Solving this equation in absence of external forces leads to the well known normal modes of oscillation of a clamped beam in vacuum with spatial profiles

$$\phi_n(x) = (\cos C_n x - \cosh C_n x) + \frac{\cos C_n + \cosh C_n}{\sin C_n + \sinh C_n}(\sin C_n x - \sinh C_n x) \tag{5}$$

where C_n is the nth solution of equation

$$1 + \cos C_n \cosh C_n = 0 \tag{6}$$

which leads to $C_1 = 1.875$, $C_2 = 4.694$, ..., $C_n = (n - 1/2)\pi$. The normals modes $\phi_n(x)$ for $n = 1, \ldots, \infty$ form an orthonormal basis of the functions of x in $[0,1]$ [16]:

$$\int_0^1 \phi_n(x)\phi_m(x)dx = \delta_{n,m} \tag{7}$$

The pulsations of these resonant modes are given by the dispersion equations

$$m_c\omega_{vac,n}^2 = \frac{C_n^4}{3}k \tag{8}$$

When the cantilever is moving inside a fluid, the force acting on the cantilever can be decomposed into 2 components: the force corresponding to the hydrodynamic load $F_{\text{hydro}}(x|\omega)$ due to the motion of the beam in the fluid, and the actual external driving $F_{\text{drive}}(x|\omega)$. Following Sader's approach [3], the hydrodynamic load can be approximated by

$$F_{\text{hydro}}(x|\omega) = \frac{\pi}{4}\rho\omega^2 b^2 \Gamma(\omega)w(x|\omega) \tag{9}$$

where $\Gamma(\omega)$ is the hydrodynamic function corresponding to the rectangular cantilever beam and ρ the density of the fluid. The real part Γ_r of Γ corresponds to the added mass due the fluid moving along with the cantilever during its motion (normalized to $m_f = \pi \rho L b^2/4$, the mass of a cylinder of fluid of diameter b and length L), and the imaginary part Γ_i to the viscous drag. To solve the equation of motion of the cantilever in the fluid, let us decompose the deflection $w(x|\omega)$ and external driving $F_{\text{drive}}(x|\omega)$ on the orthonormal basis of the normal modes ϕ_n:

$$w(x|\omega) = \sum_{n=1}^{\infty} \beta_n(\omega)\phi_n(x) \tag{10}$$

$$F_{\text{drive}}(x|\omega) = \frac{1}{L}\sum_{n=1}^{\infty} \eta_n(\omega)\phi_n(x) \tag{11}$$

We note here that this decomposition is also valid in the real time space, with amplitude $\beta_n(t)$ and external driving $\eta_n(t)$ of each mode simply being the inverse Fourier transform of $\beta_n(\omega)$ and $\eta_n(\omega)$. These 2 variables are coupled by the hamiltonian H of the system. Indeed, let us compute the infinitesimal work δW of F_{drive} when the deflection changes by δw:

$$\delta W = \int_0^1 Ldx F_{\text{drive}}(x,t)\delta w(x,t) \tag{12}$$

$$= \sum_{n=1}^{\infty} \eta_n(t)\delta\beta_n(t) \tag{13}$$

For a reversible transformation, we can write $dH = \delta W$, hence

$$\frac{\partial H}{\partial \beta_n} = \eta_n \tag{14}$$

This last equation shows that the amplitude β_n and external driving η_n of each mode are coupled variables by the hamiltonian of the system. We can thus apply the Fluctuation Dissipation Theorem [17]: the power spectrum density S_{β_n} of fluctuation of amplitude for mode n is given by

$$S_{\beta_n}(\omega) = \frac{2k_B T}{\pi \omega}\text{Im}(\frac{\beta_n(\omega)}{\eta_n(\omega)}) \tag{15}$$

where k_B is the Boltzmann constant, T the temperature of the thermostat and Im(.) is the imaginary part of its argument.

We will now explicit the right part of eq. 15. Using the orthonormalization of the base ϕ_n, we can easily show that eq. 4 leads to the following equation for each mode:

$$\left(\frac{k}{3}C_n^4 - (m_c + m_f\Gamma(\omega))\,\omega^2\right)\beta_n(\omega) = \eta_n(\omega) \tag{16}$$

The amplitude β_n of each mode is thus governed by the equation of motion of an oscillator with stiffness $kC_n^4/3$, mass $m_c + m_f\Gamma_r(\omega)$ and damping coefficient $m_f\omega\Gamma_i(\omega)$, forced by external driving η_n. If $\Gamma(\omega)$ is a slow varying function of the frequency, close to its resonance each mode behaves like an harmonic oscillator. Using the above expression, eq. 15 can be rewritten as

$$S_{\beta_n}(\omega) = \frac{2k_B T}{\pi \omega}\text{Im}(\frac{1}{\frac{k}{3}C_n^4 - (m_c + m_f\Gamma(\omega))\,\omega^2}) \tag{17}$$

$$= \frac{2k_B T}{\pi}\frac{1}{m_c}\frac{\tau\Gamma_i(\omega)\omega}{(\omega_{vac,n}^2 - (1 + \tau\Gamma_r(\omega))\omega^2)^2 + \tau^2\Gamma_i^2(\omega)\omega^4} \tag{18}$$

with $\tau = m_f/m_c$. In general, dissipation couples the modes calculated from the non-dissipative equations, but within the approximation of position independent dissipative forces (eq 9), the noises are uncorrelated. We can thus write a generic expression of the power spectrum density of the deflection using eq. 10:

$$S_w(x,\omega) = \sum_{n=1}^{\infty} S_{\beta_n}(\omega)|\phi_n(x)|^2 \tag{19}$$

This last equation is in agreement with the one derived by Dorignac et al. [7] in a more complex framework.

3 Experiment

To test the validity of the above formalism, we measure the thermal noise of a commercial AFM cantilever (Budget Sensor BS-Cont) with the following nominal geometry: $L = 450\,\mu\text{m}$, $b = 50\,\mu\text{m}$, $h = 2\,\mu\text{m}$. The cantilever is made of Silicium and is coating-less, thus for theoretical expressions we used the tabulated values of Si for the young Modulus ($E = 169\,\text{GPa}$ for Si_{110}, the usual crystalline orientation along the length of AFM cantilever) and density ($\rho_c = 2340\,\text{kg}\cdot\text{m}^{-3}$). The length and width were checked with an optical microscope, and the thickness is inferred from the resonance frequency of the cantilever (from eq. 8), which eventually leads to $L = 450\,\mu\text{m}$, $b = 48\,\mu\text{m}$, $h = 2.07\,\mu\text{m}$.

The measurement is performed with a home made interferometric deflection sensor [18], inspired by the original design of Schonenberger [19] with a quadrature phase detection technique [20]: the interferences between the reference laser beam reflecting on the base of the cantilever and the sensing laser beam on the free end of the cantilever directly gives a calibrated measurement of the deflection $w(x = 1, t)$, with very high accuracy. We illustrate in Fig.2 the performance of our detection with the power spectrum density (PSD) of a rigid mirror (in black): the background noise of our system is as low as $1.3 \times 10^{-27}\,\text{m}^2/\text{Hz}$, just $50\,\%$ higher than the shot noise limit of our detection system. Typical noise of a measurement in a commercial AFM would be at least two orders of magnitude higher.
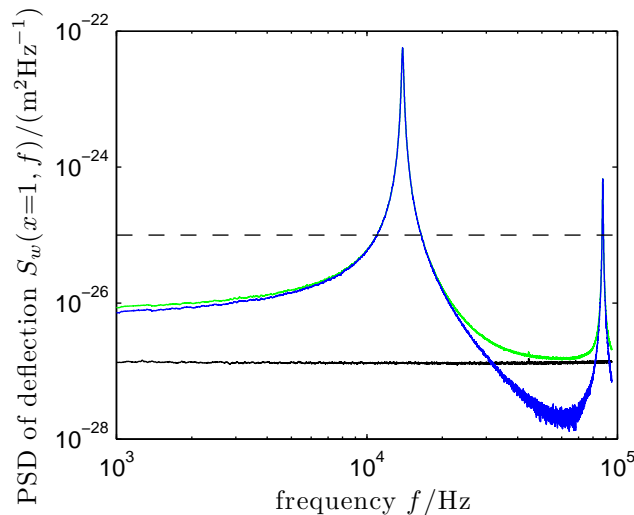

Figure 2: Power spectrum density (PSD) of deflection. The PSD of thermal noise driven deflection at the free end of the cantilever (−) is measured with an home made interferometric setup in a $1\,\text{kHz}$ to $100\,\text{kHz}$ range. We clearly see the two first flexural modes of the mechanical beam, well above the background noise of the apparatus (−) acquired on a rigid mirror. The difference between the measurement and the background noise spectrums (−) gives a full view of the behavior of the thermal fluctuations of the cantilever in this frequency window. For comparison, the typical noise floor of a well tuned and calibrated commercial AFM is plotted (- -): only the resonances could be studied, the remaining part of the spectrum would be useless.

We plot in Fig.2 the PSD of thermal noise driven deflection at the free end of the cantilever (in green). We clearly see in this spectrum the two first modes of oscillation of the mechanical beam, around $f_1 = 14\,\text{kHz}$ and $f_2 = 87\,\text{kHz}$, but we also have a lot of information out of these resonances as the measurement is always above the background noise of the system. If we subtract this background noise spectrum from the measurement (blue curve), we have an estimation of the thermal noise of the system on the whole $1\,\text{kHz}$ to $100\,\text{kHz}$ frequency interval, which we can compare to the theoretical expectation of the model presented in the previous section. The same measurement in a commercial AFM would yield much less information, as it would be limited to the resonances, and we would not have any information between them or at low frequency .

In Fig.3, we compare the measured PSD of fluctuations (in blue) with the prediction of 3 different models (in red) for the thermal noise of the cantilever, all based on Sader's approach [3]. The hydrodynamic function $\Gamma(\omega)$ used for these predictions was taken from eq. 20, 21a and 21b of ref. [3], as it correspond to the first two resonances and the extension to higher order modes of ref. [8] is not necessary. The first model (Fig.3(a)) corresponds to eq. 29a of the original article of Sader [3], where the frequency dependence of the thermal

noise forcing as been omitted. Both resonances are really well described with this model, but the off-resonance behavior is not: the low frequency noise measured is not flat as expected by the model, which also slightly underestimates the noise the intermediate region.

The second model (Fig.3(b)) corresponds to eq. 17a of ref. [8], a corrected expression of the thermal noise proposed by Green and Sader (see ref. 44 of [5]) to account for frequency dependance of the dissipation following the approach of Paul and Cross [4]. Let us first note that this expression is dimensionally incorrect, as it is homogeneous to m^2 and not to m^2/Hz, so we had to rescale the formula by $2.28 \times 10^{-4}\,Hz^{-1}$ to match the first resonance. However, this model perfectly describes the frequency dependance of the first mode, catching the slow variation of the noise in the low frequencies. The behavior of the second mode could also be well described, but it would need a higher rescaling factor.

We came to the conclusion that the scaling factor is mode dependent, and conducted the analysis of the previous part to derive the correct expression. Indeed, it can easily be shown that the frequency behavior of each mode (eq. 17) is exactly the same as in ref. [8], but the scaling factors are different. We plot in (Fig.3(c)) the prediction of eq. 17 and eq. 19, and see that we match the whole power spectrum density of fluctuation of deflection: both resonances, low frequency and intermediate region are very well described by the model. We stress here that the only parameter we have adjusted in the model is the thickness of the cantilever h, to match the actual frequencies of resonance. The Sader approach to describe the effect of the embedding fluid on the behavior of the cantilever turns out to be very good on the whole frequency range probed here.

4   Conclusion

In this paper, we have presented a simple theoretical framework to describe the thermal noise of a mechanical beam in a viscous fluid. Under the assumption of an infinitely thin and long cantilever, we used the Sader approach to describe the effect of the surrounding fluid (added mass and viscous drag). Using the fluctuation dissipation theorem for each flexural modes of the system, we derived a general expression for the power spectrum density of fluctuations as the sum of the contribution of the different modes. This prediction has been compared with an experimental measurement on a commercial AFM cantilever in a frequency range covering the 2 first resonances. A very good agreement has been found on the whole spectrum, with no adjustable parameters but the thickness of the cantilever. This analysis can be very useful in the AFM area, where the thermal motion of the cantilever is of great practical importance (as a lower bound to measurable forces or as a mechanical driving on its own): it is not limited to a fit of resonances only, but gives an *a priori* knowledge of the cantilever noise on the whole frequency spectrum.

References

[1] N. V. Lavrik, M. J. Sepaniak, and P. G. Datskos, *Review of Scientific Instruments*, 75(7):2229–2253, 2004.

[2] E. Meyer, H. J. Hug, and R. Bennewitz, *Scanning Probe Microscopy: The Lab on a Tip.* Springer, 2004.

[3] J. E. Sader, *Journal of Applied Physics*, 84(1):64–76, 1998.

[4] M. R. Paul and M. C. Cross, *Phys. Rev. Lett.*, 92(23):235501, Jun 2004.

[5] C. P. Green and J. E. Sader, *Journal of Applied Physics*, 98(11):114913, 2005.

[6] M. R. Paul, M. T. Clark, and M. C. Cross, *Nanotechnology*, 17(17):4502–4513, 2006.

[7] J. Dorignac, A. Kalinowski, S. Erramilli, and P. Mohanty, *Physical Review Letters*, 96(18):186105, 2006.

[8] C. A. Van Eysden and J. E. Sader, *Journal of Applied Physics*, 101(4):044908, 2007.

[9] M. V. Salapaka, H. S. Bergh, J. Lai, A. Majumdar, and E. McFarland, *Journal of Applied Physics*, 81(6):2480–2487, 1997.

[10] F.-J. Elmer and M. Dreier, *Journal of Applied Physics*, 81(12):7709–7714, 1997.

[11] A. Maali, C. Hurth, R. Boisgard, C. Jai, T. Cohen-Bouhacina, and J.-P. Aimé, *Journal of Applied Physics*, 97(7):074907, 2005.

[12] S. Basak, A. Raman, and S. V. Garimella, *Journal of Applied Physics*, 99(11):114906, 2006.

[13] J. W. M. Chon, P. Mulvaney, and J. E. Sader, *Journal of Applied Physics*, 87(8):3978–3988, 2000.

[14] N. A. Burnham, X. Chen, C. S. Hodges, G. A. Matei, E. J. Thoreson, C. J. Roberts, M. C. Davies, and S. J. B. Tendler, *Nanotechnology*, 14(1):1–6, 2003.

[15] M. K. Ghatkesar, T. Braun, V. Barwich, J.-P. Ramseyer, C. Gerber, M. Hegner, and H. P. Lang, *Applied Physics Letters*, 92(4):043106, 2008.

[16] K. F. Graff, *Wave motion in elastic solids.* Dover, 1975.

[17] S. R. de Groot and P. Mazur, *Non-equilibrium thermodynamics.* Dover, 1984.

[18] P. Paolino and L. Bellon, Quadrature phase interferometer for AFM measurements. *in preparation.*

[19] C. Schonenberger and S. F. Alvarado, *Review of Scientific Instruments*, 60(10):3131–3134, 1989.

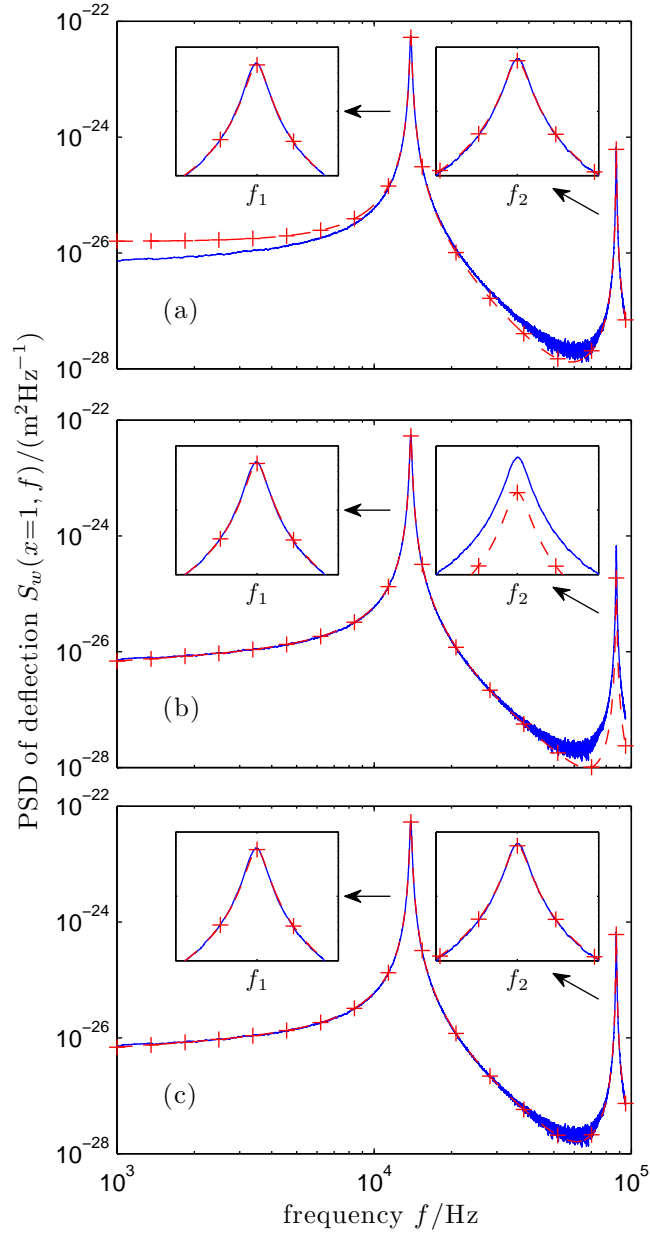[20] L. Bellon, S. Ciliberto, H. Boubaker, and L. Guyon, *Optics Communications*, 207(1-6):49–56, 2002.

Figure 3: Power spectrum density (PSD) of thermal noise driven deflection at the free end of the cantilever: measurement (—) vs 3 different models (−+−). (a) prediction after [3], (b) prediction after [8], (c) prediction from eq. 17 and eq. 19 of the present work. Insets present zooms around the resonances.